

# Suppression and Enhancement of CSR-Driven Emittance Degradation in the IR-FEL Driver

*D. Douglas*

## Abstract

We discuss the impact of coherent synchrotron radiation (CSR) on beam transported through the IR FEL driver. The mechanism for emittance degradation by CSR is reviewed, and a method of controlling this degradation is described. A computer model for simulation of CSR effects in transport systems is presented and its application to the driver transport system described. Based on simulations using this model, we find that:

1. for typical operating parameters (135 pC/bunch and nominal transport system tunings) CSR will degrade emittance on the order of 10% during transport through the system,
2. significant suppression of CSR-driven emittance degradation occurs due to symmetries inherent in the transport system design,
3. emittance degradation is, to some extent, controllable, and
4. appropriate (or, perhaps, inappropriate) adjustment of transport system attributes can result in large (order 100%) growth of emittance under certain conditions.

Transport system features leading to suppression and enhancement of CSR effects are discussed.

## Introduction

CSR is an effect of concern to those who wish to generate high brightness electron beams. This self-interaction of a bunch with its own classical radiation field leads to transverse and longitudinal emittance degradation at levels potentially rendering a transported beam useless for applications such as FELs. It is, for example, concerns about CSR [1] that led to the present IR FEL driver transport system implementation in which the wiggler is immediately downstream of the linac. The purpose of this note is to document a simple CSR model now included in DIMAD, and to discuss the results of its use in a study of means to control CSR-driven emittance degradation in the IR FEL driver transport system.

The CSR model in use throughout this discussion computes the energy shift on an electron in a bunch due to the steady-state CSR force in free space from the bunch's own classical radiation field [2]. In this model, the relative

momentum shift  $dp/p$  experienced by an electron at longitudinal position  $s$  in a Gaussian line-charge bunch of rms length  $s_s$  due to CSR generated during transport of the bunch through an angle  $\Delta q$  at bend radius  $r$  is given by the following expression.

$$\frac{dp}{p} = \left\{ \frac{18000 Q r^{1/3} \Delta q}{3^{1/3} \sqrt{2p} s_s^{4/3} E} \right\} \text{Int} \left( \frac{s}{s_s} \right)$$

Here,  $Q =$  total charge in the bunch (Coulomb),  
 $E =$  bunch central energy (MeV), and  
 $\text{Int}(s/s_s) =$  wake-field integral, which describes the CSR-induced longitudinal wake-field on the electron.

The integral can be evaluated numerically, and is shown in Figure 1 over an interval of  $\pm 10s_s$  around the bunch centroid (positive numbers are at the head of the bunch). This expression gives an estimate of the momentum shift induced on the electron

as it experiences the bunch self-field while moving through the bend. This momentum shift can, through a mechanism reviewed in the next section, induce emittance degradation by causing growth in the transverse size and angular divergence of the beam. We should note,

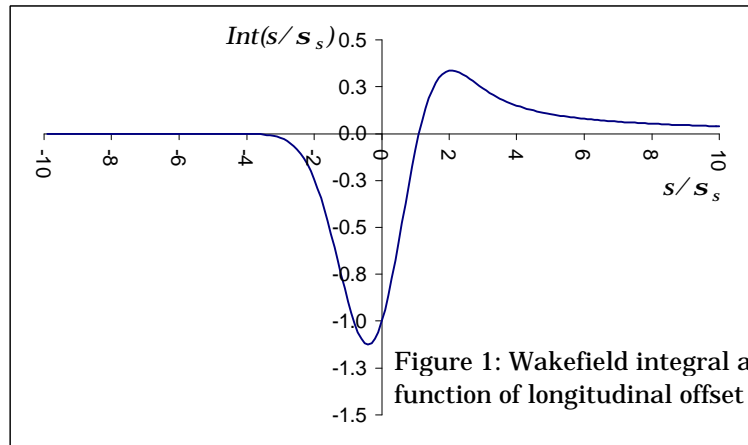


Figure 1: Wakefield integral as function of longitudinal offset

however, that the effect is a systematic one. If the electron is placed in the same position in the bunch at a location where the bunch is of the same length, it will experience the same momentum shift when bent through the same angle at the same radius. This introduces the possibility that cancellation or compensation of the effect can be arranged. This subject will be addressed below.

### CSR-Driven Emittance Degradation

The CSR-induced energy shift experienced by an electron within a bunch during bending can lead to degradation of transverse emittance. To illustrate the mechanism, we consider an electron with design energy moving on the on-momentum design trajectory. Such an electron is at the origin of the transverse phase space (illustrated in Figure 2), and thus has zero action (the

Courant/Snyder invariant, or equivalent emittance, is zero). If the electron undergoes a momentum shift  $dp/p$  due, for example, to CSR, it begins to betatron oscillate around the *off-momentum* design trajectory  $(h dp/p, h' dp/p)$ . At any undispersed point downstream, it then will have *nonzero* action – that is, the emittance will have grown, due to the energy shift at the dispersed point with the resultant betatron oscillation around the off-momentum orbit. In short, CSR causes the beam to oscillate about point A in Figure 2 – this oscillation persists, corresponding to emittance growth, even at points where the off-momentum orbit re-joins the on-momentum one.

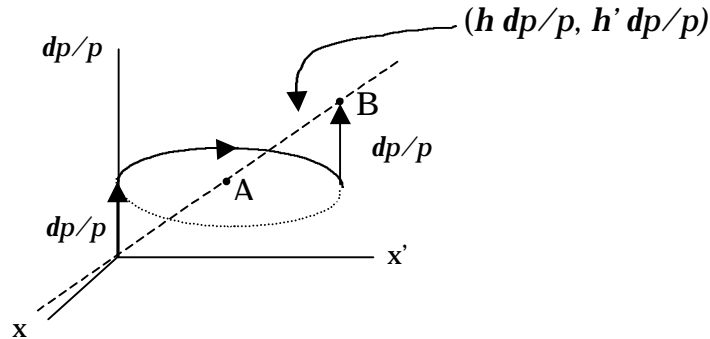


Figure 2: Mechanism for emittance degradation. An electron at the origin suffers an energy shift  $dp/p$  due to CSR, and therefore betatron oscillates about the point  $A = (h dp/p, h' dp/p)$ . If lattice functions, bunch length, and particle path length offset all reproduce at a point in an identical dipole  $180^\circ$  in betatron phase away from the initial excitation point, the electron suffers a second, *identical* energy shift  $dp/p$  due to CSR. Because this occurs while at the point  $B = (h 2dp/p, h' 2dp/p)$ , the CSR energy impulse moves the electron *onto* the appropriate off-momentum orbit, suppressing the betatron oscillation.

A mechanism for suppression of the CSR-driven excitation then suggests itself [4]. We arrange the transport so that it is periodic, with half-integer phase advance between two identical periods, which have in addition isochronous transport separating them. In such a case, the electron will arrive at the second period at the same longitudinal position as it had when at the first period. Consequently, the electron experiences a CSR-driven excitation in the second period identical to that it received in the first. Recall, however, that the electron has been betatron oscillating about the off-momentum orbit due to CSR excitation in the first period, and is, due to the selected phase advance, *already on the off-momentum orbit for the momentum displacement to which it is moved by CSR in the second period!* The CSR kick in the first period and betatron phase advance from the first to the second

period move the electron to point B in Figure 2. This is *exactly* where it needs to be so that the CSR kick in the second period moves it onto the design orbit associated with its new momentum offset. The second CSR kick thus eliminates the action induced by the first kick; the electron is on the appropriate off-momentum orbit and the emittance degradation is cancelled!

This cancellation is a synchro-betatron analog to the suppression of geometric aberrations in second-order achromats with non-interleaved sextupoles. The key points are that

1. there be transverse symmetry – the betatron and dispersion functions at the “homologous” lattice points should be identical
2. there be a appropriate phase relationship – the betatron phase advance between homologous lattice points should be a half integer
3. the transport between homologous points should be such that the bunch length is the same, and each electron is at the same position within the bunch, at both points. This can be achieved through use of isochronous individual periods and isochronous transport from period to period.

As we will see in the following discussion of the IR FEL driver, a sufficient (though perhaps tighter than necessary) condition to ensure cancellation is that the beam line consist of two identical achromatic, isochronous periods the starting (and hence ending) points of which are separated by a half-betatron wavelength. Another scheme that would also result in suppression is the use of a second-order achromat with isochronous individual periods.

Several things can interfere with this suppression. First, the phase advance (and other transfer map properties, such as momentum compaction) between homologous lattice points will, in general, depend on momentum offset; the cancellation will therefore be imperfect due to chromatic (and geometric) aberrations. As the momentum is different from the design value, the electron will not return to precisely the same phase space location (either transversely or longitudinally), so that the compensating CSR-induced momentum shift will not be exactly the same as the initial CSR-induced shift. Use of the second-order achromat based scheme mentioned in the previous paragraph would assist in overcoming this difficulty.

A second problem with suppression stems from the fact that a single electron will not experience an individual kick that is to be compensated at a single downstream point; rather, CSR continuously shifts the electron energy as it is transported through the beam line. The resultant compensation will therefore be limited by higher-order terms due to cross-couplings between energy shifts all along the beam line. In the language of the second-order-achromat analogy, CSR excitation/suppression occurs in systems that

correspond to use of interleaved, rather than non-interleaved, sextupoles, and are thus subject to the influence of higher-order effects. These will manifest themselves as residual emittance growth values that depend nonlinearly on bunch charge (just as the residual geometric aberrations in an interleaved second-order achromat depend quadratically on sextupole strength).

A final imperfection in compensation will occur in any beam with nonzero emittance by virtue of the fact that  $M_{51}$  and  $M_{52}$  are nonzero throughout a system with dispersion. Thus, the electron path length from the initial excitation point to the compensation point will deviate (by  $M_{51}X+M_{52}X'$ ) from the initial value leaving the electron at a different longitudinal position within the bunch. This leads to a different CSR-driven energy shift than that imposed initially. It has in fact been suggested [4] that transverse beam size could be used to “turn off” CSR – by increasing the bunch size to values large compared with the radiation wavelength, the coherence could be eliminated and the effect suppressed.

## Modeling of CSR

The free-space CSR model described above has been put into DIMAD [5] as an arbitrary element. The element is to be used in tracking computations for tracing rays. It is implemented by interleaving it with slices of a sub-divided bend magnet; each time the CSR element is called, it gives each particle a momentum kick modeling the CSR excitation driven by transport through a dipole slice by using the expression detailed above. The model then continues on to the next beam-line element. The element is input at the MAD level; the syntax is as follows.

```
name:arbitelm,l=0,p1=onoff,p2=charge,p3=rho,p4=angle,p5=energy
```

Here,

name	is the CSR element name used in the DIMAD beamline definition,
l=0	is the length assigned to the element – set to zero meters inasmuch as this is an impulsive kick,
p1=onoff	a toggle to turn CSR off and on; +1 for on, -1 for off,
p2=charge	the single bunch charge in Coulomb,
p3=rho	the bend radius [m] in the previous dipole slice,
p4=angle	the bend angle [degrees] of the previous dipole slice, and
p5=energy	the beam central energy, [MeV], in the previous dipole slice.

Computation is quite fast with little obvious slow-down in code execution when CSR is activated. The only subtlety in coding was that the above model

has  $s > 0$  corresponding to the head of the bunch; DIMAD has  $dl < 0$  corresponding to the head – so a change of sign was required. Procedurally, the code uses a lookup table (the same used to produce Figure 1) to evaluate the CSR kick. When first called, it evaluates the rms bunch length, then loops over all particles. For each particle, the program interpolates the wake-field integral at the particle longitudinal position using the lookup table, then evaluates the momentum kick using the above expression and the parameters passed in the element definition. The  $\pm 10s$  span of the lookup table was set to allow use of  $\pm 6s$  Gaussian-distributed bunches during tracking simulations; a  $\pm 5s$  full span occasionally encountered out of range particles during tracking, the  $\pm 10s$  full span has so far avoided this.

The program, by stepping through slices of the dipole, thus effectively integrates the impact of CSR on each particle within the bunch, and, by subsequent tracking, determines the impact of the transport on downstream CSR effects. Results of simulations using this model are discussed in the following section.

### **Results for IR FEL Driver**

The above tool has been applied to the IR FEL driver to understand features of CSR production in the transport system and to ascertain the impact of CSR in typical operating situations. Two numerical tests were performed. The first test was a simple *benchmark* to verify that the code was properly evaluating the above formula and to determine if the aforementioned suppression scheme could work. The second test was a more involved *parametric scan* of beam performance as a function of CSR-related parameters. In all tests, tracking was done from point of tangency to point of tangency (essentially, 2F09 to about 5F05). The transport was set to be achromatic and isochronous in each of the two end arcs. The 2F04-2F09 matching telescope was adjusted at the outset to match beam envelopes into the recirculation arcs – beam envelopes at the centers of both C bends are identical, the slopes are zero, and the transport is reflectively symmetric about the center of the backleg

*Benchmark* – To benchmark the CSR model and to test compensation of emittance degradation, a simple test case was executed by tracing a limited number of rays. A pseudo-Gaussian line-charge bunch containing 19 particles (all on the transverse central orbit, distributed as in Figure 2 longitudinally, and injected at the design momentum) was tracked through the driver energy recovery transport (from point of tangency to point of tangency) with CSR activated. Results were first manually spot-checked using the above formula; DIMAD was found to properly evaluate the momentum shift for each particle, indicating that the code was properly constructed.

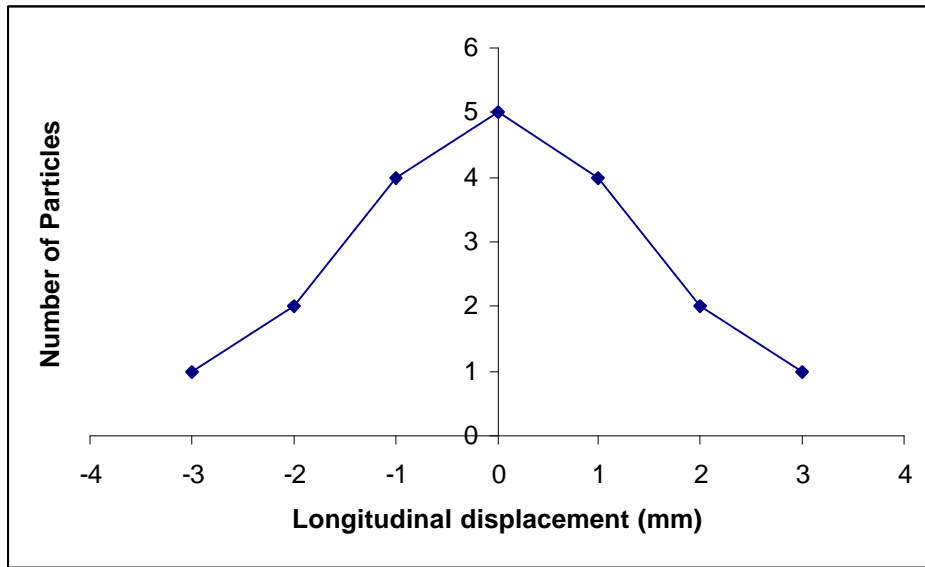


Figure 2: Pseudo-Gaussian test distribution of 19 particles.

To test the CSR suppression hypothesis, the phase advance from C-bend center to C-bend center was set to either 2.5 or 3 betatron wavelengths and the beam envelopes re-matched (to be unchanged in the arcs proper) using the backleg quadrupoles in a reflectively symmetric arrangement. The bunch charge was varied by powers of 2, from 33.75 pC to 540 pC. At each bunch charge and for each phase advance, the single particle action (Courant/Snyder invariant) was computed for each particle at the end of each arc proper.

We find for low charges (up to 135 pC, but *not* 270 pC), the action grows quadratically with bunch charge at the end of the 1<sup>st</sup> arc. This is as expected – the CSR driven momentum shift is linear in the charge per bunch; each of the  $x$  and  $x'$  so generated (*via* the local dispersion) are therefore also linear, meaning the action will be quadratic in charge. Thus for example, at 33.75 pC the average action is  $\sim 0.5$  nm-rad, while at 67.5 pC it is  $\sim 2$  nm-rad. For a full-wavelength separation between the C-bends, the action tends to increase  $\sim 20\%$  in the second arc and the remnant value (after the arc) again varies as charge squared. Thus for example at 33.75 pC the average remnant action is  $\sim 0.64$  nm-rad; at 67.5 pC it is  $\sim 2.5$  nm-rad. However, for a half-wavelength separation between the C-bends, the remnant action decreases dramatically (3 orders of magnitude!) and varies as charge to the *fourth*. Thus, for example, at 33.75 pC the average remnant action is 0.5 pm-rad; at 67.5 pC it is 8 pm-rad.

These results indicate that suppression of emittance growth does occur as conjectured above. Note, however, for high charge states (270 to 540 pC) the suppression breaks down. This may be due to the cross coupling effects (between CSR momentum kicks) discussed above.

*Parametric scan* – A ray-tracing exercise was performed to determine the parametric dependence of emittance performance with CSR activated. A Gaussian bunch of 10,000 particles (at 42 MeV central energy) was generated with a  $\pm 6\sigma$  cutoff in all phase space dimensions. A 13 mm-mrad normalized emittance ( $\sim 0.16$  mm-mrad geometric emittance at 42 MeV) was used, as were matched beam envelope functions and a longitudinally upright phase space with rms bunch length of 0.3 mm and rms relative momentum spread of  $10^{-3}$ . This was tracked through the recirculation transport (from point of tangency to point of tangency) for single bunch charge states of 60, 135, 270 and 540 pC with phase advances (from center of C-bend to center of C-bend) of 2,  $2\frac{1}{4}$ ,  $2\frac{1}{2}$ ,  $2\frac{3}{4}$ , 3,  $3\frac{1}{4}$ , and  $3\frac{1}{2}$  wavelengths. In each case, the beam was rematched (using a symmetric arrangement of the backleg quadrupoles) to keep the beam envelopes unchanged and reflectively symmetric across the backleg and in the arcs, which, as noted above, were individually achromatic and isochronous.

Results are presented in Figure 3, which shows the horizontal emittance following each arc (“middle” and “end”) after tracking a bunch with various charge states through the lattice at multiple phase advances. As the phase advance variation effects only the end-to-end transport, we naturally see no phase dependence in the results after the first arc. The “middle” emittance does, however, exhibit the quadratic dependence on bunch charge discussed above. The emittance at the end of the beam line shows a sinusoidal dependence on phase advance, with degradation at a maximum when the centers of the C-bends are separated by a full betatron wavelength and at a minimum when they are separated by a half-wavelength. The quadratic dependence of the degradation on bunch charge is also apparent at some level, even with half-wavelength phase advances. It appears that the geometric and chromatic effects discussed above do indeed impede exact suppression of first arc emittance growth by the second arc. We observe at most only slight reduction of the “middle” emittance by the second arc, except in the case of very high charge state bunches. Finally, we note that for nominal driver parameters (135 pC, half-wavelength phase advance), the anticipated emittance growth after both arcs is at the few mm-mrad level, or only about 10%.

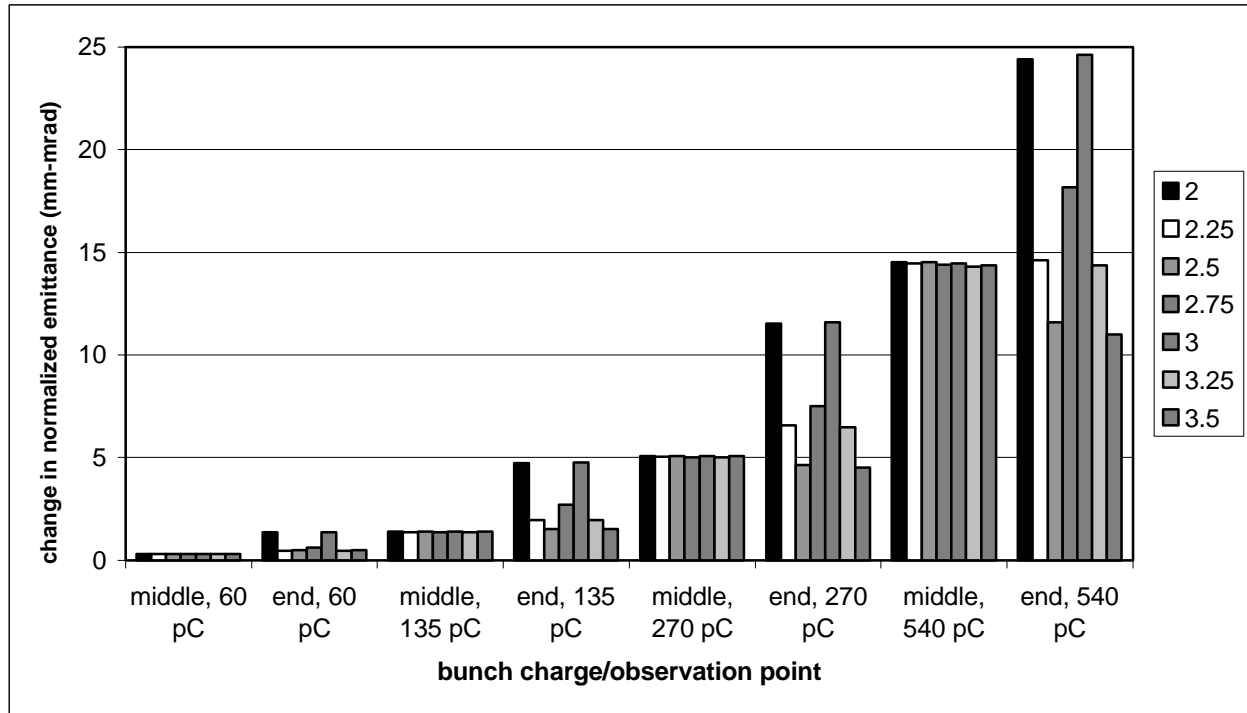


Figure 3: Horizontal emittance of 10,000-particle bunch of various charge states after tracking through beam line with various phase advances. “Middle” refers to observation point after first arc; “end” refers to observation point after second arc.

### Enhancement of CSR Effects

The above discussion suggests that CSR dilution of emittance is of little practical concern in the IR FEL driver. For proper choice of phase advance, the effect can be limited to  $\sim 1$  mm-mrad growth of an initial 13 mm-mrad injected normalized emittance, which is well within the system acceptance. As the effect arises downstream of the wiggler, it will have little operational impact.

Future FEL drivers will however have tighter constraints on emittance budgets and/or will, to improve compactness, locate wigglers in the machine backleg. It is therefore useful to understand and demonstrate control over CSR effects in the present driver. To this end, we have investigated scenarios in which nominally small CSR effects in the driver can be enhanced so as to be both more readily observed and to demonstrate theoretical understanding of, and empirical control over, this phenomenon. In the following, we discuss how the suppression mechanism discussed above is manifested in the driver design and describe ways in which this mechanism can be circumvented so as to enhance the impact of CSR. We note that in the above study, the “design” beam emittance of 13 mm-mrad was used. This is an upper limit on the

allowable emittance (as it is the largest value allowing third harmonic lasing [6]), but is somewhat larger than the emittance anticipated from nominal machine performance. To obtain results consistent with present operational expectations (as well as to [hopefully!] increase the *relative* magnitude of the effect) we use, in the following, a smaller value of 8.4 mm-mrad for the normalized emittance. This translates to a geometric emittance of 0.1 mm-mrad at 42 MeV, the nominal operating energy of the recirculator. As in the above discussion, the following study uses a longitudinally upright bunch of 0.3 mm length and 0.001 relative momentum spread as an initial condition.

The Bates arc on which the recirculator is based possesses multiple symmetries which suppress of CSR effects through the mechanism discussed above. The nominal tuning used above (betatron matching into the arc, isochronous transport, and a half-betatron wavelength horizontal phase advance from center of C-bend to center of C-bend) has beam envelopes and dispersions as displayed in Figure 4; Figure 5 presents betatron phase advances for this tuning.

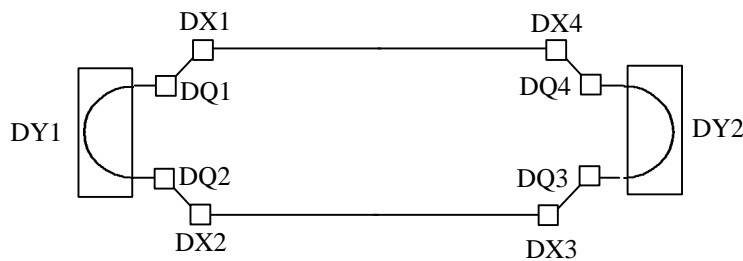
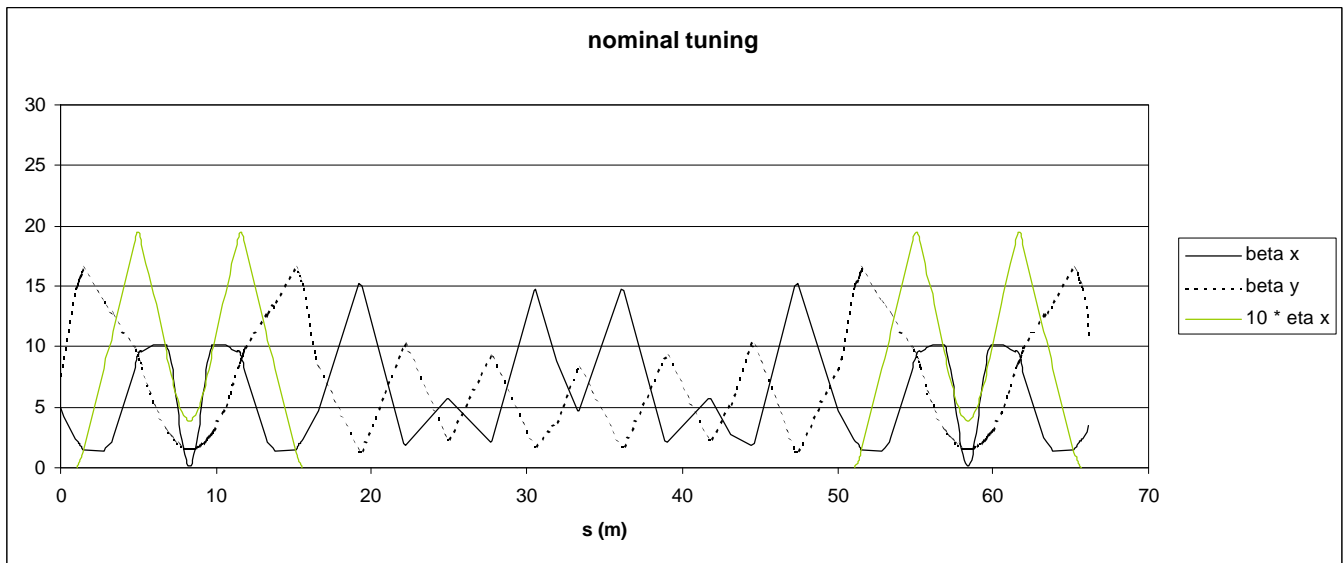


Figure 4: Beam envelopes and dispersions for nominal recirculator tuning.

Figure 5: Betatron phase advances through recirculator for nominal tuning: all dipoles paired with half wavelength separations – DY1 to DY2, DQ1 to DQ2 and DQ3 to DQ4 (due to presence of 180° bends), DX1 to DX3, and DX2 to DX4. In addition, DQ1/DQ3, DQ2/DQ4 pairings are separated by half-wavelengths due to choice of betatron phase advance.

The periodicity in these functions is evident. We note that there are 3 major dipole families – DX, DQ, and DY – and, in the nominal tuning, the beam envelopes are the same in all members of a given family. Moreover, each dipole is (modulo) a half-betatron wavelength away from a partner dipole. In the nomenclature of Figure 5, DQ1 and DQ2 are separated by DY1 and thus are a half-wavelength apart. DQ3 and DQ4 are similarly phase-related across DY2. DY1 and DY2 are separated by  $2\frac{1}{2}$  wavelengths through the choice of phase advance (selected, recall, so as to suppress CSR effects). This choice of phase advance (set by the backleg) coupled with the nominal phase advance of the end loops leads to similar suppressive half wavelength phase advances between both the DX1/DX3 pair and the DX2/DX4 pair. In addition, the DQ1/DQ3 and DQ2/DQ4 pairs are separated by modulo a half-wavelength. The nominal tuning thus is quite self-suppressive with respect to CSR effects.

Using this tuning with the beam properties described above, a DIMAD simulation of recirculation with CSR leads to a final emittance of  $\sim 0.123$  mm-mrad, or about 20% growth (corresponding to 1.7 mm-mrad growth in normalized emittance).

To modify the CSR-driven emittance growth, we shifted the C-bend center to C-bend center phase advance to 3 betatron wavelengths. According to the above discussion, this should enhance, rather than suppress, CSR effects. To facilitate comparison to the half-wavelength result, the beam envelopes were held constant in the arcs; this was accomplished by rematching using recirculator backleg quadrupoles in a reflectively symmetric arrangement. The resulting beam envelopes are shown in Figure 6; phase advances are displayed in Figure 7.

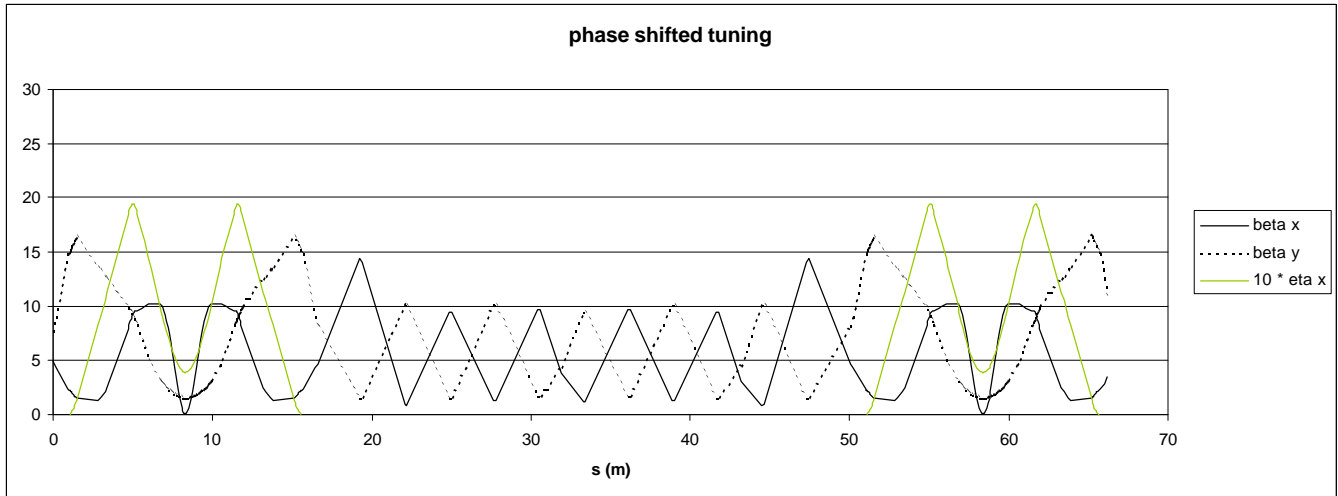


Figure 6: Beam envelopes and dispersions for phase-shifted tuning.

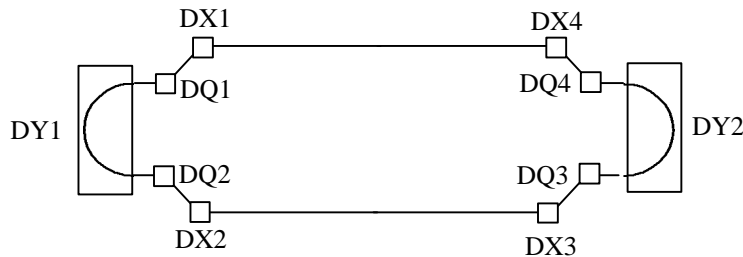


Figure 7: Betatron phase advances for phase-shifted tuning: many dipoles paired with full wavelength separations – DY1 to DY2, DX1 to DX3, and DX2 to DX4. In addition, though DQ1/DQ2 and DQ3/DQ4 pairs are still about a half wavelength apart (due to presence of  $180^\circ$  bends), the DQ1/DQ3 and DQ2/DQ4 pairs are a full wavelength apart.

Periodicity of envelopes and dispersions in all dipoles is again evident. Note however that only the DQs are now separated by half-betatron wavelengths [7]; all other families lie (modulo) a full betatron apart. As discussed above, this should enhance CSR-driven emittance growth. This is in fact confirmed by simulation; the resulting final emittance is  $\sim 0.167$  mm-mrad, a  $2/3$  growth in the geometric emittance. This corresponds to  $\sim 5$  to  $6$  mm-mrad growth in the normalized emittance.

In search of further CSR enhancement, we developed a recirculator tuning deliberately violating beam envelope, dispersion, and momentum compaction periodicity and, in addition, shifting phase advances amongst various dipole family members so as to avoid suppression of CSR effects. This was done by creating a dispersion wave across the backleg using the trim quadrupoles and

rematching from arc to arc using the backleg quadrupoles in a reflectively symmetric array to zero the beam envelope and dispersion slopes in the center of the backleg. The resulting tuning removes virtually all periodicity in beam envelope functions at homologous dipoles, shifts the momentum compaction (thereby assuring the path lengths of various particles do not match well from arc to arc), and leads to a set of phase advances which do not contribute to suppression of CSR effects. Beam envelopes are shown in Figure 8; phase advances are displayed in Figure 9.

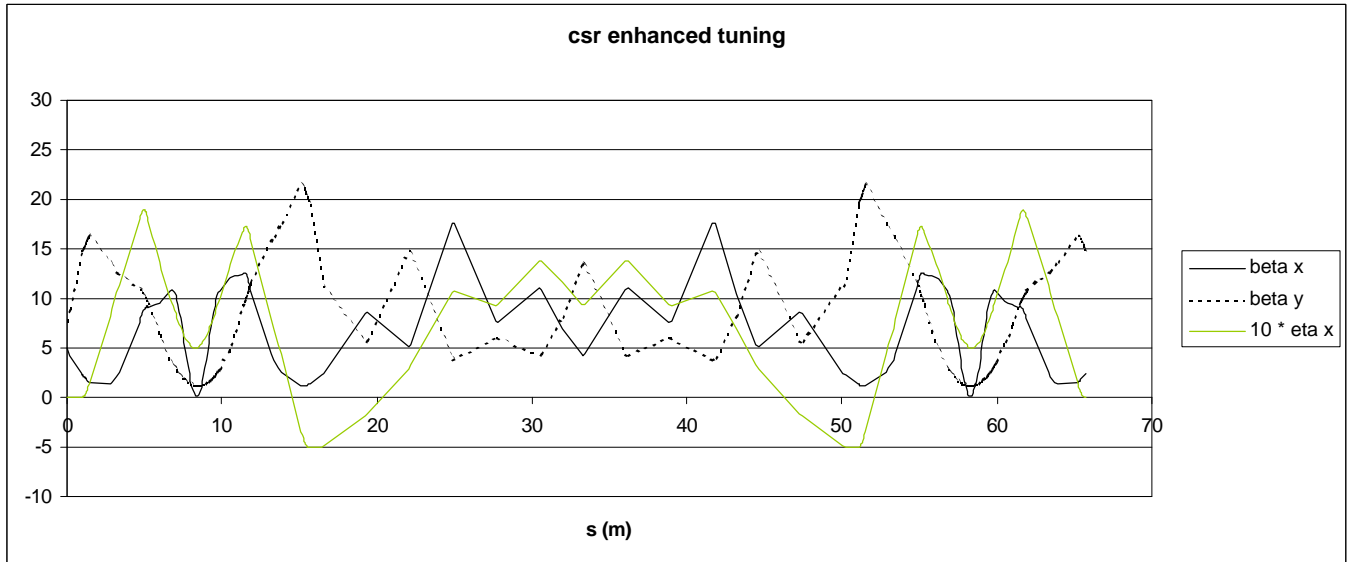


Figure 8: Beam envelopes and dispersions for CSR-enhanced tuning.

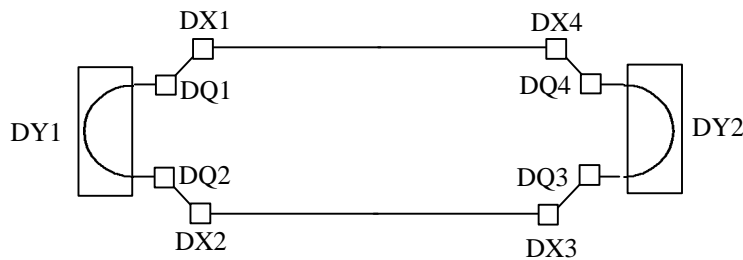


Figure 9: Betatron phase advances for CSR-enhanced tuning: before, DQ1/DQ2 and DQ3/DQ4 pairs are split by a half-wavelength. Here, DY1/DY2 are separated by a quarter wavelength, and the DX pair at points with equal beam envelopes are all separated by a full or quarter wavelength. CSR effects therefore tend to add.

The absence of periodicity in beam envelopes and dispersions at all dipoles is evident. The DQs do, by virtue of their arrangement around the DYs, CSR self-suppress. The deviations of beam envelopes and dispersions amongst the DXs, and the phase advance between the DYs, limit any CSR suppression amongst these elements. This is born out by DIMAD simulation, which indicates the final beam emittance will be  $\sim 0.2$  mm-mrad. This corresponds to a 100% growth of emittance – a change of about 8 mm-mrad in normalized emittance.

This tuning, moreover, appears to admit emittance measurements upstream of the reinjection point using a standard monitor/quad scan technique. This will require only installation of a single OTR or other profile monitor at the reinjection point.

Further studies on this topic are in progress. They are, first, aimed at verifying the practicality of emittance measurements upstream of reinjection while using these tunings. Secondly, development of tunings that allow observation of significant CSR effects in the backleg are underway. We note that the geometry of the Bates design is such that any configuration leading to significant CSR growth in a single end loop will almost certainly require the measurement of emittances at with dispersion present in the backleg. Techniques suggested for use in CEBAF are under investigation in this context [8].

## **Conclusions**

A simple CSR model is now available in DIMAD for use as a design tool.

Use of this model suggests that CSR-driven emittance growth will not be a significant issue in the operation of the IR FEL driver.

The model has been used to verify that suppression of CSR effects can be achieved through proper choice of phase advances and momentum compactions amongst dipoles with appropriately periodic beam envelope and dispersion functions.

CSR effects in the IR FEL driver can be enhanced in an operationally practical manner. The enhancement can as much as double the anticipated injected emittance, with the result readily observable using standard diagnostic techniques.

## Acknowledgements

I would like to thank Rui Li for providing the details of the CSR model and Joe Bisognano for assistance in understanding these details, for the suggestion for investigating “half-betatron-wavelength suppression” of CSR-driven emittance degradation, and for providing significant motivation and quality assurance for this work. I would also like to thank Geoff Krafft and Court Bohn for several useful and informative discussions on this topic.

## References

- [1] C. Bohn, private communication.
- [2] R. Li provided the details of this model (including formulae and numerical tables). This description was drawn from various sources, including Ya. S. Derbenev, J. Rossbach, E. L. Saldin, and V. D. Shiltsev, “Microbunch Radiative Tail-Head Interaction” and Ya. S. Derbenev and V. D. Shiltsev, “Transverse Effects of Microbunch Radiative Interaction”, FERMILAB-TM-1974/SLAC-Pub 7181, May 1996.
- [3] Or, more accurately, is suggested by J. Bisognano.
- [4] G. Krafft, private communication.
- [5] R. Servranckx *et al.*, “User’s Guide to the Program DIMAD”, SLAC Report SLAC-285, UC-28 (A), May 1985.
- [6] A Bensonism.
- [7] This is unavoidable, inasmuch as the DQ pairs are each separated by a DY and are therefore necessarily a half-wavelength apart.
- [8] D. R. Douglas and D. V. Neuffer, “High Power Emittance and Momentum Spread Measurements Using Endstation Transport Lines”, CEBAF-TN-93-092, 23 November 1993.